33rd Annual International Conference of the IEEE EMBS
Boston, Massachusetts USA, August 30 - September 3, 2011

Mathematical, Numerical and Experimental Study in the Human Aorta with Coexisting Models of Bicuspid Aortic Stenosis and Coarctation of the Aorta

Z. Keshavarz-Motamed, J. Garcia, L. Kadem

Abstract—**Coarctation of the aorta is an obstruction of the aorta and is usually associated with other concomitant cardiovascular abnormalities especially with bicuspid aortic valve stenosis. The objectives of this study are, (1) to investigate the effects of coarctation on the hemodynamics in the aorta to gain a better understanding of the cause of certain post-surgical coarctation problems, (2) to develop and introduce a new lumped parameter model, mainly based on non-invasive data, allowing the description of the interaction between left ventricle, coarctation of the aorta, aortic valve stenosis, and the arterial system.**

I. Introduction

Coarctation of the aorta (COA) is a common cardiovascular condition, accounting for 5%–10% of congenital heart disease and represents 7% of critically ill infants with heart disease [1]. However, the existing parameters to evaluate the severity of COA are mainly flow dependent and have significant limitations [2, 3]. Even after successful intervention, recoarctation after angioplasty estimated to occur in up to 40% of patients after intervention, post-surgical hypertension exists in 11% to 68% of patients and development of aneurysm after patch graft repair are common. Despite their significant preponderance, the exact mechanisms of the post surgery problems are still not completely understood. Numerous investigations pointed out that there is a relationship between the genesis and the progression of cardiovascular disease and the locally irregular flow occurring at the diseased zone [4].

Furthermore, COA often occurs in combination with bicuspid aortic stenosis (AS) (20 to 85%) [5]. In this case, the left ventricle (LV) faces a double-pressure-overload: AS + COA. This leads to a major increase in left ventricular work. Therefore, assessment of the left ventricular stroke work which is the energy that the ventricle delivers to the blood at ejection, and potential energy, necessary to overcome the viscoelastic properties of the myocardium itself is fundamental in understanding cardiovascular pathophysiology and therapeutics, especially for heart failure. The use of pressure-volume analysis has been established as a powerful means of characterizing ventricular pump properties at end systole, end diastole, and throughout the entire cardiac cycle independent of loading conditions [6]. However, this parameter requires invasive determination of the instantaneous ventricular pressure and volume, thus limiting its in vivo application. Under such conditions, it is highly important to determine total load supported by the LV and to decouple the respective impacts of AS and COA on the left ventricle function in order to predict which load is the most significant hence making decision of clinical treatment by valve replacement and/or COA surgery.

The objective of this study, therefore, is a joint mathematical, numerical and experimental study in an anatomical aorta with both bicuspid AS and COA with the following aims, (1) investigation of blood flow dynamics to understand the hemodynamic factors that lead to acute and gradual changes in the function and health of vessels, (2) investigation of the respective impacts of AS and COA on the left ventricular load to provide surgeons more insight on the LV load since it has been shown to effectively characterize patient's outcome.

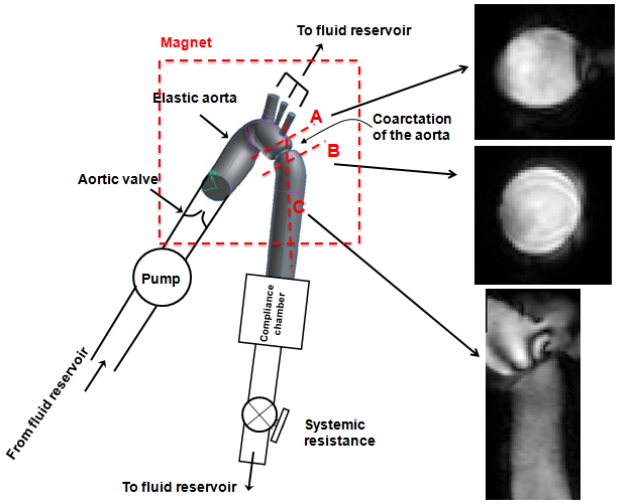

Fig. 1. Schematic diagram of the in vitro flow model used for MRI measurements. Dashed red lines show three planes measured with MRI.

II. Methodology

A. Experimental study

The in vitro model used for magnetic resonance imaging (MRI) measurements includes a fluid reservoir, a gear pump,

Z. Keshavarz-Motamed, Mechanical and Industrial Engineering, Concordia University, Montréal, Canada (Corresponding author's email: z_kesha@encs.concordia.ca)
J. Garcia, Québec Heart and Lung Institute, Laval University, Québec, Canada
L. Kadem, Mechanical and Industrial Engineering, Concordia University, Montréal, Canada

elastic models of the aorta (healthy aorta and COA including: ascending aorta, aortic branches and descending aorta) and adjustable systemic arterial resistance and compliance (Fig.1). The fluid (65% saline and 35% glycerin used to mimic viscous proprieties of blood) is pumped from a reservoir, crosses the aortic valve and then is directed towards the aortic branches and the descending aorta. Instantaneous flow rates were measured by T206 Transonic flowmeter (Transonic System Inc., Ithaca, NY, USA, accuracy of 1% full scale) at the level of descending aorta and aortic arch arteries.

The aortic model was placed at the center of the magnet during the tests and all data were collected with the use of a clinical 3 Tesla magnetic resonance scanner with a dedicated phase-array receiver coil (Achieva, Philips Medical Systems, Best, Netherlands). An ECG patient simulator (model 214B, DNI Nevada Inc, USA) was used to synchronize scanner gating with the PC controllable pump. A standard examination was performed by initial acquisition of SSFP cine images in standard longitudinal and transversal planes for acquisition planning. MRI imaging parameters consisted of: TR/TE (17.99/3.97ms), flip angle (15°), pixel spacing (1.66 mm), slice thickness (10 mm), acquisition matrix (256 x 256) and encoding velocity (2 × maximal velocity).

Simplified continuity equation was used to compute effective orifice area (EOA) under pulsatile flow for both COA and AS used in the experiment as follow,

$$EOA = SV / VTI_{AO} \quad (1)$$

where SV is the stroke volume determinate by Simpson's rule upstream to the COA (or AS) and VTI_{Ao} is the velocity-time integral of maximal velocities downstream from the COA (or AS) in the aortic section. We obtained effective orifice areas of 1.71 cm^2 and 1.03 cm^2 for COA and AS, respectively.

A custom-made research application was developed using Matlab software (Mathworks, Natick, Ma) to process and analyze all MRI images.

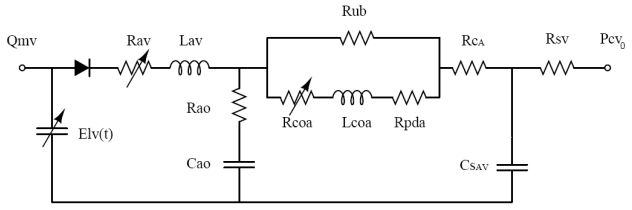

Fig. 2. Schematic diagram of the lumped parameter model with concomitant of aortic stenosis and coarctation of the aorta.

B. Numerical simulations

Computations were performed using open source computational fluid dynamics toolbox (OpenFOAM) based on a finite volume method. In the healthy vessels, the blood flow is usually laminar and does not experience transition to turbulence. Therefore, the solution was obtained by simulating a laminar flow inside the domain of healthy aorta. The obstruction resulting from a stenosis and/or coarctation can lead to disturbed flow regions in the aorta. Hence, in this study, the model with both COA and BAV has been investigated using the transitional version of the $\kappa-\omega$ turbulence model [7] (Fig.1). COA model is symmetric with severity of 75% by area. Blood was assumed to be a Newtonian and incompressible fluid with dynamic viscosity of 0.0035 Pa·s and density of 1050 kg/m^3 [8]. The assumption of a Newtonian fluid behavior is realistic for blood flow in large arteries like the aorta as the shear rates in large arteries are sufficiently large [8]. Mesh independency was judged by two criteria: velocity and wall shear stress. Mesh independency was achieved for these two criteria for all cases with 2,166,000 and 1,335,000 elements for aorta with COA and BAV and healthy aorta, respectively. For time independency, several time steps were tested: 0.001 s, 0.002 s and 0.0025 s and 0.003 s. The solution finally marched in time with a time step 0.0025 s. The convergence was obtained when all residuals reached a value lower than 10^{-5}.

Table 1. Summary of the cardiovascular parameters used

Systematic circulation parameters		
Aortic resistance	R_{ao}	0.05 mmHg.s.ml-1
Aortic compliance	C_{ao}	0.5 ml/mmHg
Systemic vein resistance	R_{SV}	0.05 mmHg.s.ml-1
Systemic arteries and veins compliance	C_{SAC}	2 ml/mmHg
systemic arteries resistance (including arteries, arterioles and capillaries)	R_{CA}	0.8 mmHg.s.ml-1
Upper body resistance	R_{ub}	Adjusted to have 15% of total flow rate in healthy case
Proximal descending aorta resistance	R_{pda}	0.05 mmHg.s.ml-1
Output condition		
Central venous pressure	P_{CV0}	4mmHg
Input condition		
Mitral valve mean flow rate	Q_{mv}	
Other		
Constant blood density		1050 kg/m3
Cardiac output	CO	5.2 l/min
Heart rate	HR	70 beats/min
Duration of cardiac cycle	T	0.857 s

C. Lumped parameter model

A schematic diagram of the lumped parameter model developed and used in this study is presented in Fig.2 including left heart-arterial model, AS model and COA model. The net instantaneous pressure gradient through the COA and AS is as follow [9].

$$TPG_{net} = \frac{2\pi\rho}{\sqrt{E_L Co}}\frac{\partial Q(t)}{\partial t} + \frac{\rho}{2E_L Co^2}Q^2(t) \quad (2)$$

Where E_LCo, EOA and Q are the energy loss coefficient, the effective orifice area and the flow rate, respectively. Verification of the lumped parameter model in presence of AS and COA was done with in vivo MRI measurements from the literature [10, 11]. The coupling between LV pressure and LV volume is performed through a time varying elastance E(t) and the arterial system as follow.

Where $P_{LV}(t)$, V(t) and V_0 are left ventricular pressure, left ventricular volume and unloaded volume, respectively. Summary of all other cardiovascular parameters used in this

study is in the table1.

$$E(t) = \frac{P_{LV}(t)}{V(t) - V_0} \quad (2)$$

Lumped parameter model illustrated in figure 2 was analyzed numerically by creating and solving system of ordinary differential equations in Matlab Simscape (MathWorks, Inc). Capabilities of this program were enhanced by adding additional codes to meet demands of cardiac model in circuit. Equation 1, representing the transvalvular pressure gradient across the AS and the COA, was represented by an inductance and a variable resistor as depicted in figure 2. Simulation starts at the onset of isovolumic contraction and elastance signal drives the program by feeding elastance value related to each time step in the cycle to the equation 1. Convergence residual criterion was set to 10^{-5} with initial time step of 0.1 milliseconds and initial voltages and currents of capacitors and inductors set to zero.

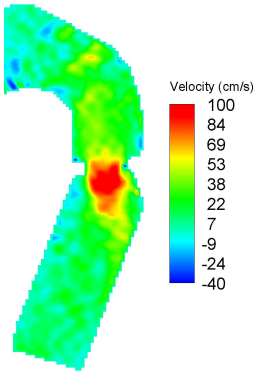

Fig. 3. Axial velocity contour at COA during acceleration (plane C) resulted from MRI

(a) (b)

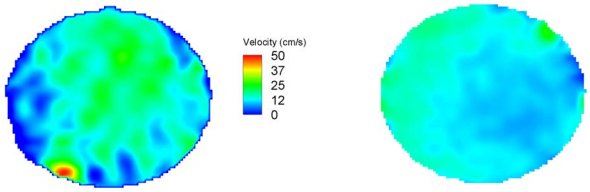

Fig. 4. Velocity contours of the cross section A during acceleration resulted from MRI, (a) COA, (b) normal

(a) (b)

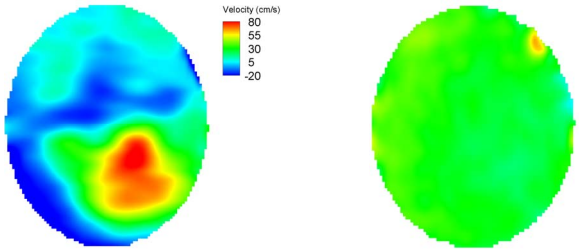

Fig. 5. Velocity contours of the cross section B during deceleration resulted from MRI, (a) COA, (b) normal

III. Results and Discussions

Figure 3 shows that as the flow exits the COA, the fluid cannot abruptly change the direction and follow the steep curvature of the coarctation. The disturbed flow resulted from COA detached from the walls and developing into a jet which has a peak axial velocity of 100 cm/s (demonstrating 5 times the normal value: 20 cm/s) achieved during acceleration at about 0.5 of coarctation diameter downstream of the COA (called vena contracta). Also maximum axial velocity does not occur on the centerline anymore but instead a skewed velocity profile develops where higher velocities occur near the wall during systole as also reported by [12]. This is of paramount interest because in normal aorta, the typically laminar flow is fully attached and streamlines are skewed smoothly towards the inner wall during early systole. The magnitude of the axial velocity profile was relatively low (with a magnitude of 20 to 30 cm/s). Furthermore, there is almost no flow reversal occurring except at very late systole, which is very minimal.

Figures 4 and 5 show that the COA has a significant effect on velocity contours upstream and downstream of the COA (planes A and B). Presence of this flow restriction changes the rather uniform velocity profile of the normal case (No COA and No AS) in figures 4.b and 5.b to the complicated velocity fields of figures 4.a and 5.a. This alteration is more manifested downstream of the COA where negative velocities demonstrating vortices are present.

(a) (b)

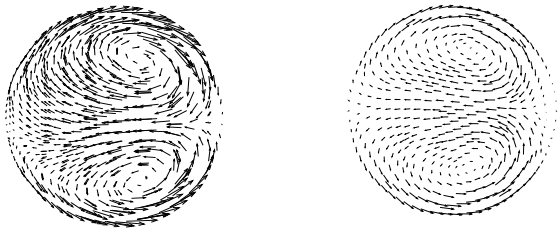

Fig. 6. secondary flow at the cross section B during deceleration resulted from numerical simulations, (a) COA, (b) normal

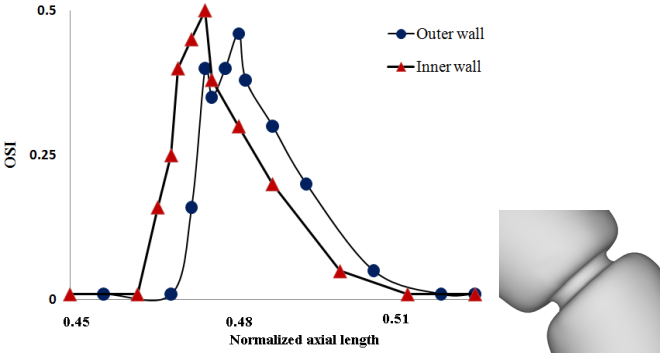

Fig.7. OSI at the inner and outer wall of COA region

Figure 6 shows that secondary flows became stronger leading occupying almost the whole section as a result of COA. Downstream of the COA, it clearly appeared that the COA amplified even more the secondary flows and a strong jet-like flow going from the inner wall towards the outer wall can be noticed. It appeared that as a result of elevated axial velocity and centrifugal force, the counter-rotating vortices developed in COA are convected towards the inner wall. This new configuration of the secondary flow in

compare to normal case will have a significant impact on the wall shear stress distribution at the inner wall.

Due to the pulsatile nature of blood flow in arteries, the oscillatory character of shear stress is important to analyze [13]. Fig. 7 shows the oscillatory shear index (OSI) distribution which has a range between 0 and a maximum of 0.5, where 0.5 indicates entirely oscillatory flow. The numerical results, then, suggest that high OSI values of up to 0.50 can be seen at downstream of the COA. Areas of high OSI lie within the areas of flow reversal or varying flow direction which are considered to be more susceptible to intimal thickening and plaque formation [13].

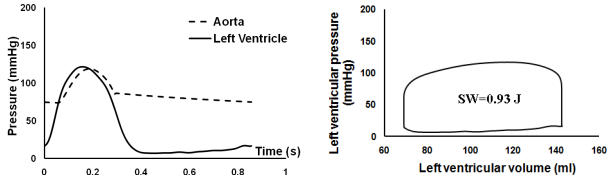

LV peak pressure = 120 mmHg

Fig. 8. Simulated left ventricular and aortic pressure and stroke work resulted from lumped model (normal case: no AS and no COA)

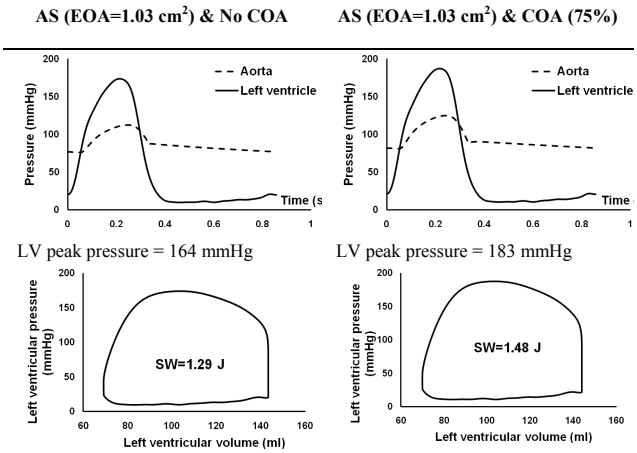

Fig. 9. Simulated left ventricular and aortic pressure and stroke work resulted from lumped parameter model

Left ventricular and aortic pressure and stoke work were computed by using lumped parameter model (Fig. 2) (EOA of COA= 1.71cm^2 and EOA of AS= 1.03 cm^2 resulted from MRI). Figure 9 reveals that both COA and AS will act like a localized resistance by shifting up the pressure waveforms. The COA (EOA=1.71 cm^2) and bicuspid AS (EOA=1.03 cm^2) increase LV pressures by 20 mmHg and 44 mmHg, respectively. This has an instantaneous effect on the LV stroke work which increases from 0.93 J (No AS and No COA) (Fig. 8) to 1.29 J (AS and No COA) and finally to 1.48 J (both AS and COA) (Fig. 9). Under such conditions, if the valve is replaced, this patient would not fully benefit from aortic valve replacement if no COA surgery was planned, since LV stroke work would remain abnormally high. This operation corrects the valvular component of the left ventricular afterload but not its vascular component related to COA. For the same case, repairing only the COA will lead to a decrease in the LV stroke work from 1.48 J to 1.29 J.

IV. Conclusion

The results showed that the coexistence of both pathologies has a significant impact on the flow in the aorta and indicate significant variation across the COA lesion. This study also reveals the respective impacts of aortic stenosis and coarctation of the aorta on the left ventricular stroke work. The suggested model can be used to predict which load is the most significant hence making decision of clinical treatment by valve replacement and/or COA surgery and to predict the outcome for such patients.

V. Acknowledgement

Authors appreciate helps of MRI Laboratory at Universidad Autonoma Metropolitana-Iztapalapa, Mexico City, Mexico.

References

[1] F. Secchi, A. Iozzelli, G. D. E. Papini, A. Aliprandi, G. Di Leo, F. Sardanelli, "MR imaging of aortic coarctation," *Radiol med*, vol. 114, pp. 524-537, 2009.

[2] J. C. Steffens, M. W. Bourne, H. Sakuma, M. O'Sullivan, C. B. Higgins, "Quantification of collateral blood flow in coarctation of the aorta by velocity encoded cine magnetic resonance imaging," *Circulation*, vol. 90, pp.937-943, 1994.

[3] J. S. Caravalho, A. N. Redington, E. A. Shinebourne, M. Rigby, D. Gibson, "Continuous wave Doppler echocardiography and coarctation of the aorta: gradients and flow patterns in the assessment of severity," *Heart*, vol. 64, pp. 133-137, 1990.

[4] A. Frydrychowicz, et al., "Multidirectional flow analysis by cardiovascular magnetic resonance in aneurysm development following repair of aortic coarctation," *J Cardiovasc Magn Reson.* 10:30, 2008.

[5] H. B. Grotenhuis, A. D. Roos, "Structure and function of the aorta in inherited and congenital heart disease and the role of MRI," *Heart*, vol. 97, pp. 66-74, 2011.

[6] K. Sagawa, W. L. Maughan, H. Suga, K. Sunagawa, " Cardiac contraction and the pressure-volume relationship," Oxford: Oxford Univ. Press, 1988.

[7] F. Ghalichi, X. Deng, A. D. Champlain, Y. Douville, M. King, R. Guidoin, "Low Reynolds number turbulence modeling of blood flow in arterial stenosis," *Biorheology*, vol. 35, pp. 281–94, 1998.

[8] L. Morris, et al. "3-D numerical simulation of blood flow through models of the human aorta," *Biomech*, vol. 127, pp.767–775, 2005.

[9] D. Garcia, P. Pibarot, L. G. Durand, "Analytical modeling of the instantaneous pressure gradient across the aortic valve," *J. Biomech*., vol. 38, pp. 1303-1311, 2005.

[10] M. Markl, et al., "Three dimensional flow characteristics in aortic coarctation and poststenotic dilatation*," Journal of Computer Assisted Tomography,* vol. 33, no.5, pp. 776-778, 2009.

[11] M. D. Hope, et al., "Clinical evaluation of aortic coarctation with 4D flow MR imaging," *Journal of Magnetic Resonance Imaging*, vol. 31, pp. 711–718, 2010.

[12] Z. Keshavarz-Motamed, L. Kadem, "3D pulsatile flow in a curved tube with coexisting model of aortic stenosis and coarctation of the aorta" *Med Eng Phys*, vol. 33, pp. 315-324, 2011.

[13] D. N. Ku, D. P. Giddens, C. K. Zarins, S. Glagov, "Pulsatile flow and atherosclerosis in the human carotid bifurcation: positive correlation between plaque location and low and oscillating stress," *J. Arterioscler*, vol. 5, pp. 292–302, 1985.